Video Article

Evaluating Targeting Accuracy in the Focal Plane of an Ultrasound-guided High-intensity Focused Ultrasound Phased-array System

Ke Li[1,2], Jingfeng Bai[1,2], Yazhu Chen[1,2], Xiang Ji[1,2]

[1]Biomedical Instrument Institute, School of Biomedical Engineering, Shanghai Jiao Tong University

[2]Shanghai Med-X Engineering Center for Medical Equipment and Technology, Shanghai Jiao Tong University

Correspondence to: Jingfeng Bai at jfbai@sjtu.edu.cn, Xiang Ji at xiangji@sjtu.edu.cn

URL: https://www.jove.com/video/59148
DOI: doi:10.3791/59148

Keywords: Ultrasound-guided high-intensity focused ultrasound (USgHIFU), phased array, targeting accuracy, marker, phantom

Date Published: 12/18/2018

Citation: Li, K., Bai, J., Chen, Y., Ji, X. Evaluating Targeting Accuracy in the Focal Plane of an Ultrasound-guided High-intensity Focused Ultrasound Phased-array System. *J. Vis. Exp.* (), e59148, doi:10.3791/59148 (2018).

Abstract

Phased arrays are increasingly used as high-intensity focused ultrasound (HIFU) transducers in the existing extracorporeal ultrasound-guided HIFU (USgHIFU) systems. The HIFU transducers in such systems are usually spherical in shape with a central hole where a US imaging probe is mounted and can be rotated. The image on the plane of treatment can be reconstructed through the image sequence acquired during the rotation of the probe. Therefore, the treatment plan can be made on the reconstructed images. In order to evaluate the targeting accuracy in the focal plane of such systems, the protocol of a method using a bovine muscle and marker-embedded phantom is described. In the phantom, four solid balls at the corners of a square resin model serve as the reference markers in the reconstructed image. The target should be moved so that both its center and the center of the square model can coincide according to their relative positions in the reconstructed image. Swine muscle with a thickness of about 30 mm is placed above the phantom to mimic the beam path in clinical settings. After sonication, the treatment plane in the phantom is scanned and the boundary of the associated lesion is extracted from the scanned image. The targeting accuracy can be evaluated by measuring the distance between the centers of target and lesion, as well as three derivative parameters. This method cannot only evaluate the targeting accuracy of the target consisting of multiple focal spots rather than a single focal spot in a clinically relevant beam path of the USgHIFU phased-array system, but it can be also used in the preclinical evaluation or regular maintenance of USgHIFU systems configured with phased-array or self-focused HIFU transducer.

Introduction

The phased array is increasingly designed and equipped in HIFU systems[1,2,3,4,5,6,7]. In USgHIFU phased-array systems, a US imaging probe is usually mounted in the central hole of the spherical HIFU transducer[1,2,8]. The probe is rotatable for targeting and image reconstruction in the three-dimensional space[9]. Precise targeting is required for the safety and efficacy of HIFU treatment. However, most of the studies for the evaluation of targeting accuracy have been performed for magnetic resonance-guided HIFU systems or USgHIFU systems configured with a self-focused HIFU transducer[10,11,12,13,14,15,16]. The purpose of the method described below is to evaluate the targeting accuracy in the focal plane for USgHIFU phased array systems.

A bovine muscle/marker-embedded phantom along the clinically relevant beam path is used in the evaluation of the targeting accuracy of a clinical USgHIFU phased-array system. A square model with four balls at the corners is fabricated and embedded, in combination with bovine muscle, into the transparent phantom. A regular hexagon is selected as the target based on the positions of the centers of four balls identified in the reconstructed US image on the treatment plane. After HIFU sonications, the treatment plane of the phantom is scanned, and the boundary of the lesion, as well as the positions of the four balls, can be determined in the scanned image. The targeting accuracy can be evaluated by measuring the distance between the centers of target and lesion, as well as three derivative parameters.

The method is simpler than the measurement of the targeting error using robotic movement with a specific reference object[11,17,18] and more clinically relevant in comparison to the method based on single focal spot ablation in a homogeneous phantom[10]. This method can be used in the evaluation of the targeting accuracy of USgHIFU phased array systems. It can be also used for other USgHIFU systems equipped with self-focused HIFU transducers.

Protocol

1. Marker design and fabrication

1. Design a square model using computer-aided design software. Set each side as sticks with lengths of 40 mm and thicknesses of 2 mm. Place a solid ball with a 10 mm diameter at each corner of the square model.
2. Use acrylonitrile butadiene styrene photosensitive resin as the material for printing.
3. Send the 3D model file to a manufacturer for fabrication.

2. Phantom preparation

1. Attach a plastic cylinder (with a diameter of 8 cm and a height of 3 cm) to an acrylic baseboard with silica gel to make a phantom holder at room temperature. Let it sit for 1 h.
2. Slice fresh bovine muscle into a square shape (30 mm x 30 mm, with a thickness of 10 mm) and ventilate it for 2 h to evaporate moisture.
3. Pour degassed and deionized water (115 mL) in a beaker, add in 13 g of acrylamide, and stir until dissolved. Add 0.24 g of bis-acrylamide and stir until dissolved. Then, add 0.2 mL of N,N,N',N'-tetramethylethylenediamine and stir uniformly.
   NOTE: Put on a mask and rubber gloves.
4. Prepare 5 mL of degassed and deionized water in another beaker, add 0.3 g of ammonium persulfate, and stir to dissolve.
   CAUTION: Acrylamide, bis-acrylamide, N,N,N',N'-tetramethylethylenediamine, and ammonium persulfate are toxic. Pay close attention and avoid physical contact.
5. Successively pour 40% of the solutions from steps 2.3 and 2.4 into the phantom holder, and stir for 5 s. Let the mixture sit for 20 min to solidify.
6. Place the 3D-printed square model on the surface of the solidified phantom, and put the sliced bovine muscle in the middle of the model. Pour the rest of the solution from step 2.3 into the phantom holder. Move the bovine muscle back and forth to remove the air between the interface of the phantom and the slice.
7. Pour the rest of the solution prepared in step 2.4 into the phantom holder, and stir for 5 s.
8. Fine-tune the location of the sliced bovine muscle to the center of the phantom along the transverse direction. Let it sit for 20 min to solidify the phantom.
9. Remove the silica gel between the cylindrical plastic and the acrylic baseboard, using a screwdriver.
10. Slowly detach the acrylic baseboard from the cylindrical plastic.

3. Setup of the USgHIFU system

1. Start the clinical USgHIFU system.
2. Turn on the water-processing module, and set the speed of water circulation at 80 rounds/min.
3. Fill an acrylic cylindrical water tank (with a diameter of 30 cm and a height of 13 cm) with degassed water at room temperature (22-25 °C).
4. Place the phantom holder into the degassed water and fix the holder tightly.
5. Move the cylindrical water tank onto the treatment bed. Lift the treatment bed and move it down the therapeutic unit into the degassed water.

4. US-guided targeting

1. Move the therapeutic unit slowly up and down to make sure that the depth of the treatment plane is located at the upper interface of the sliced bovine muscle and transparent phantom in the US image.
2. Rotate the US imaging probe to 0° and move the cylindrical water tank to make the rotating axis (also referred to as imaging axis) pass through the middle point of the two parallel sticks in the US image.
3. Rotate the imaging probe to 90° and move the cylindrical water tank to make the rotating axis pass through the middle point of the two parallel sticks in the US image.
4. Reconstruct the US image in the treatment plane at the depth of geometric focus.
5. Check if the four balls are clearly shown in the reconstructed US image and whether the target is located at the center of the square model.
   NOTE: The center of the target is predetermined at the center of the reconstructed image. The ball is determined by a circle with a 10 mm diameter, the average gray value of which is highest in a 15 mm x 15 mm square. The center of the square model is determined by the diagonal of the four balls in the reconstructed image.
6. Move the water tank according to the relative positions between the target and the square model, and repeat steps 4.4 and 4.5.
7. Lift the therapeutic unit and put the swine muscle with a thickness of around 30 mm above the phantom. Then, move down the therapeutic unit until the depth of geometric focus is 3 mm beneath the upper surface of the sliced bovine muscle.
   NOTE: The 3 mm focal correction along the beam path is estimated according to the thickness of the swine muscle based on the empirical formula from a previous study[19].

5. HIFU sonication

1. Select the following sonication parameters: pulse duration (400 ms), duty cycle (80%), acoustic power (400 W), and cooling time between the sonication of successive focal spots (30 s).
2. Set the exposure time for the focal spots in the target.
   1. Repeat the procedure for three concentric regular hexagonal targets with respective diagonals of 5.4 mm, 9 mm, and 12.6 mm. Set exposure times of 2.0 s, 2.5 s, and 3.0 s for the focal spots located at the inner, middle, and outer hexagon, respectively, and 2.0 s for the focal spot at the geometric center of the phased array.
3. Start the sonication and put one foot on the foot pedal for HIFU sonication.
4. Observe the change of echogenicity in the US image until the sonications are completed.

6. Evaluation of the targeting accuracy of the USgHIFU phased-array system

1. Fetch the phantom holder, and smoothly press the phantom to take it out.
2. Split the phantom along the treatment plane using a knife.
3. Scan the treatment plane of the phantom that contains the sliced bovine muscle.
4. Process the scanned image using mathematical software and extract the boundaries of the target and lesion.

5. Calculate the intercenter distance d_c and the maximal overshooting of the target boundary d_b.
   NOTE: d_c is the distance between the centers of the target and its respective lesion. d_b is the maximum overshooting distance between the boundary of the lesion and its respective target.
6. Compute the ratio of the areas of lesion inside and outside the target to the target area as $\eta_I = (S_A \cap S_P) / S_P$ and $\eta_O = (S_A - S_A \cap S_P) / S_P$, respectively.
   NOTE: S_P indicates the target area, S_A represents the lesion area.

Representative Results

We made phantoms dedicated to evaluating the targeting accuracy of a clinical USgHIFU phased-array system with the targets of three different sizes. **Figure 1** displays the US image at angles of 0° and 90°. The interfaces are clear, and the sticks of the square model are bright in the US images. **Figure 2** demonstrates the reconstructed US image in the treatment plane and the focal spots of the largest target. The centers of the four balls were determined by the blue circles of the same size with the highest averaged grey value. **Figure 3** shows the scanned images of the treatment plane of the phantom and the extracted boundaries of the targets and lesions.

We were able to evaluate the targeting accuracy in the focal plane according to the parameters of d_c, d_b, η_I, and η_O defined in section 6 of the protocol. The experiments were repeated three times for each target. The results are presented in **Table 1.**

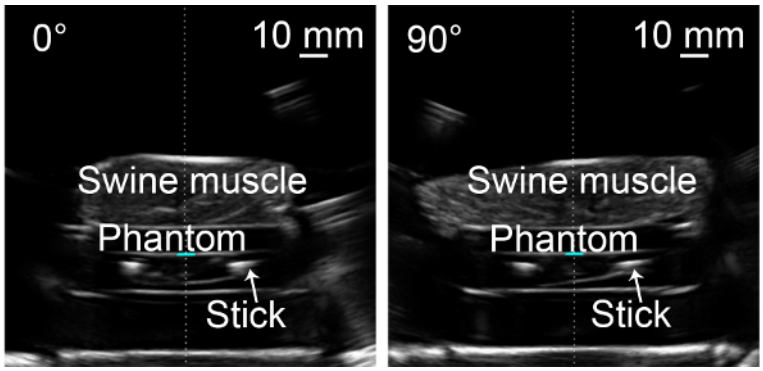

Figure 1: US images at angles of 0° and 90°. The thickness of the swine muscle was around 30 mm. The tissue-phantom-tissue interfaces along the beam path can be distinguished. Please click here to view a larger version of this figure.

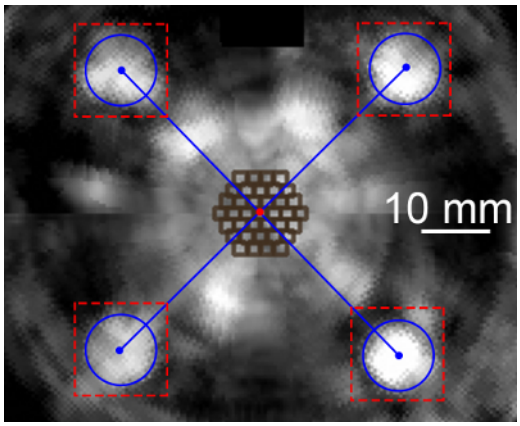

Figure 2: Reconstructed US image in the treatment plane. The blue circles (with the highest average grey value in red-dashed squares) determine the positions of four balls and the center of the square model, which is also the center of the targets (the red spot). The dark brown squares indicate the focal spots in the largest regular hexagonal target. Please click here to view a larger version of this figure.

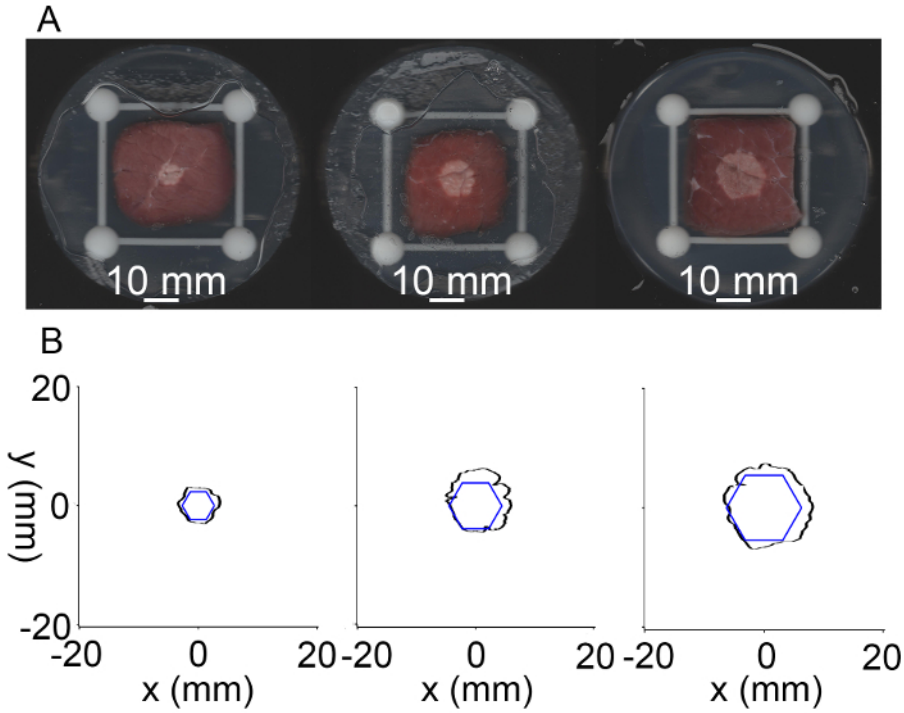

Figure 3: Scanned images and extracted boundaries of different targets after HIFU sonication. (**A**) Lesions of the three targets with diagonals of 5.4 mm, 9 mm, and 12.6 mm from left to right. (**B**) Extracted boundaries of the three targets (blue) and the corresponding lesions (black). Please click here to view a larger version of this figure.

Diagonal of regular hexagon (mm)	d_c(mm)	d_b(mm)	η_I	η_O
5.4	0.6 ± 0.3	1.6 ± 0.3	100 ± 0%	45 ± 11%
9.0	0.9 ± 0.3	1.7 ± 0.6	98 ± 1%	40 ± 6%
12.6	1.1 ± 0.4	1.7 ± 0.7	96 ± 3%	20 ± 6%

Table 1: Summary of parameters to evaluate the targeting accuracy. The values of d_c, d_b, η_I, and η_O were expressed as mean ± standard deviation.

Discussion

Robotic components have been used for extracorporeal USgHIFU systems. To evaluate the targeting accuracy of such systems, reference markers[11,12,18], in vitro tissue[17], tumor-mimic models, and temperature-sensitive phantoms have been used alone or in combination[10,20]. Compared with the protocols in those studies, this method is more clinically relevant and makes it easy to quantify the targeting error in the focal plane. By combining the reference marker with the heterogeneous, transparent phantom, this method has been modified from another study for assessing the targeting accuracy of an USgHIFU system aimed at breast tumor ablation[21]. We have verified the efficacy of this method with our USgHIFU phased-array system used on uterine fibroids in the previous study[22]. We have performed tests without focal correction along the beam path, and only a small part (~2 mm in length) of the lesion was found in the sliced bovine muscle. After the focal correction based on the empirical formula[19], the lesion (~5 mm in length) was found in the sliced bovine muscle, which has confirmed the improvement in the targeting accuracy along the beam path. Moreover, the evaluation of targeting accuracy in the focal plane is of more practical value in comparison to the methods aimed at the accuracy of a single focal spot for solid tumor ablation.

The selection of bovine muscle makes the lesion clearly distinguishable from the surrounding tissue as compared with lesions created in porcine or chicken muscles by in vitro HIFU ablation. The making of the bovine muscle/marker-embedded transparent phantom is critical for the whole protocol of evaluating the targeting accuracy of the USgHIFU phased-array system. In addition, the determination of whether the centers of the target and the square model coincide is essential in the evaluation procedure ; thus, the position of the phantom needs to be adjusted. The white intramuscular septum in the sliced bovine muscle makes the threshold segmentation insufficient to extract the lesion boundary from the scanned image; therefore, manual segmentation should be used when necessary.

There are still limitations to this protocol. This study aims for the evaluation of targeting accuracy in the focal plane only, and it is applicable to USgHIFU phased-array systems. However, for USgHIFU systems with a self-focused transducer, steps 4.2-4.4 of the protocol should be revised. The US image in the treatment plane can be reconstructed through the images acquired by translating the US imaging probe instead of by rotation, and the other steps in the protocol remain the same. The precise evaluation of targeting accuracy can be helpful when trying to reduce the safety margin and increase the ablation volume, which would improve the treatment efficacy. Moreover, this method can be used in the quality assurance of the HIFU driving system.

Disclosures

Xiang Ji is a paid consultant for Zhonghui Medical Technology (Shanghai) Co., Ltd. The other authors have nothing to disclose.

Acknowledgements

This work has been supported in part by the National Natural Science Foundation of China (81402522), the Shanghai Key Technology R&D Program (17441907400) from the Science and Technology Commission of Shanghai Municipality, and Shanghai Jiao Tong University Medical Engineering Research Fund (YG2017QN40, YG2015ZD10). Zhonghui Medical Technology (Shanghai) Co., Ltd. is also acknowledged for providing the USgHIFU system. The authors thank Wenzhen Zhu and Junhui Dong for the phantom preparation and their assistance in the experiments.

References

1. Wang, S. B., He, C. C., Li, K., Ji, X. Design of a 112-channel phased-array ultrasonography-guided focused ultrasound system in combination with switch of ultrasound imaging plane for tissue ablation. *2014 Symposium on Piezoelectricity, Acoustic Waves, and Device Applications (SPAWDA).* 134-137 (2014).
2. Choi, J. W. et al. Portable high-intensity focused ultrasound system with 3D electronic steering, real-time cavitation monitoring, and 3D image reconstruction algorithms: a preclinical study in pigs. *Ultrasonography.* **33** (3), 191-199 (2014).
3. Hand, J. W. et al. A random phased array device for delivery of high intensity focused ultrasound. *Physics in Medicine and Biology.* **54** (19), 5675-5693 (2009).
4. Khokhlova, V. A. et al. Design of HIFU transducers to generate specific nonlinear ultrasound fields. *Physics Procedia.* **87**, 132-138 (2016).
5. Melodelima, D. et al. Thermal ablation by high-intensity-focused ultrasound using a toroid transducer increases the coagulated volume. results of animal experiments. *Ultrasound in Medicine and Biology.* **35** (3), 425-435 (2009).
6. McDannold, N. et al. Uterine leiomyomas: MR imaging-based thermometry and thermal dosimetry during focused ultrasound thermal ablation. *Radiology.* **240** (1), 263-272 (2006).
7. Köhler,M. O. et al. Volumetric HIFU ablation under 3D guidance of rapid MRI thermometry. *Medical Physics.* **36** (8), 3521-3535 (2009).
8. Lu, M. et al. Image-guided 256-element phased-array focused ultrasound surgery. *IEEE Engineering in Medicine and Biology Magazine.* **27** (5), 84-90 (2008).
9. Tong, S., Downey, D. B., Cardinal, H. N., Fenster, A. A three-dimensional ultrasound prostate imaging system. *Ultrasound in Medicine and Biology.* **22** (6), 735-746 (1996).
10. Sakuma, I. et al. Navigation of high intensity focused ultrasound applicator with an integrated three-dimensional ultrasound imaging system. *Medical Image Computing and Computer-Assisted Intervention.* 133-139 (2002).
11. Masamune, K., Kurima, I., Kuwana, K., Yamashita, H. HIFU positioning robot for less-invasive fetal treatment. *Procedia CIRP.* **5**, 286-289 (2013).
12. Li, K., Bai, J. F., Chen, Y. Z., Ji, X. The calibration of targeting errors for an ultrasound-guided high-intensity focused ultrasound system. *2017 IEEE International Symposium on Medical Measurements and Applications (MeMeA).* 10-14 (2017).
13. Ellens, N. P. K. et al. The targeting accuracy of a preclinical MRI-guided focused ultrasound system. *Medical Physics.* **42** (1), 430-439 (2015).
14. McDannold, N., Hynynen, K. Quality assurance and system stability of a clinical MRI-guided focused ultrasound system: Four-year experience. *Medical Physics.* **33** (11), 4307-4313 (2006).
15. Gorny, K. R. et al. MR guided focused ultrasound: technical acceptance measures for a clinical system. *Physics in Medicine and Biology.* **51** (12), 3155-3173 (2006).
16. Kim, Y. S. et al. MR thermometry analysis of sonication accuracy and safety margin of volumetric MR imaging-guided high-intensity focused ultrasound ablation of symptomatic uterine fibroids. *Radiology.* **265** (2), 627-637 (2012).
17. Chauhan, S., ter Haar, G. FUSBOT^{US}: empirical studies using a surgical robotic system for urological applications. *AIP Conference Proceedings.* **911**, 117-121 (2007).
18. An, C. Y., Syu, J. H., Tseng, C. S., Chang, C. J. An ultrasound imaging-guided robotic HIFU ablation experimental system and accuracy evaluations. *Applied Bionics and Biomechanics.* **2017**, 5868695 (2017).
19. Li, D. H., Shen, G. F., Bai, J. F., Chen, Y. Z. Focus shift and phase correction in soft tissues during focused ultrasound surgery. *IEEE Transactions on Biomedical Engineering.* **58** (6), 1621-1628 (2011).
20. N'Djin, W. A. et al. Utility of a tumor-mimic model for the evaluation of the accuracy of HIFU treatments. results of in vitro experiments in the liver. *Ultrasound in Medicine and Biology.* **34** (12), 1934-1943 (2008).
21. Tang, T. H. et al. A new method for absolute accuracy evaluation of a US-guided HIFU system with heterogeneous phantom. *2016 IEEE International Ultrasonics Symposium (IUS).* 1-4 (2016).
22. Li, K., Bai, J. F., Chen, Y. Z., Ji, X. Experimental evaluation of targeting accuracy of an ultrasound-guided phased-array high-intensity focused ultrasound system. *Applied Acoustics.* **141**, 19-25 (2018).

